

SAR Distribution for a Strongly Coupled Resonant Wireless Power Transfer System

Xingyi Shi¹, Benjamin H. Waters¹, Joshua R. Smith^{2,1}

[1]Electrical Engineering Department [2]Computer Science and Engineering Department
University of Washington, Seattle, WA 98195

Abstract—Tissue heating is a key safety consideration in wireless power transfer (WPT) systems. Heating is regulated in the form of specific absorption rate (SAR) limitations to prevent dangerous conditions when wireless power transfer is used in proximity to people. Implanted biomedical devices which depend on wireless power transfer for their operation are particularly of interest, as a high potential for tissue heating exists in these systems. Finding ways to reduce SAR for a given load power requirement enables reduced tissue heating and/or increased limits on power transmission. This work explores SAR heating in the two resonant modes (in-phase and out-of-phase) of a strongly coupled wireless power transfer system, where the power receiver is implanted in tissue. Results based on full EM simulation with realistic planar transmit/receive coil model near 13.56 MHz and simplified tissue model indicate that the higher frequency mode (out-of-phase mode) of strongly coupled wireless power transfer results in significantly lower peak and average SAR heating.

I. INTRODUCTION

There is an increasing body of research focused on wirelessly-powered implanted medical devices and health monitoring sensors utilizing near-field magnetically coupled resonators. As a result of the increased interest in these systems, concerns about the safety of wearers of such devices have been raised, and specifically focus around the interaction of high electromagnetic (EM) fields in the human body. Although safety standards regulating human EM exposure have been established by the International Commission on Non-Ionizing Radiation Protection (ICNIRP) and the IEEE in terms of specific absorption rate (SAR), many of these studies have not been fully adopted by federal regulatory bodies for near-field wireless power system.

While a plane-wave model can be used to approximate the EM field in the far-field region, the model for the near-field region is more difficult as the electric (E) field and magnetic (H) field patterns are more complicated so power density is not appropriate to restrict exposure limit [1]. Furthermore, when the transmit coils of a near-field WPT system are strongly coupled (also known as over-coupled), the resonant system splits into two resonant modes, meaning that it has two efficiency peaks at two splitting frequencies [2]. The SAR distribution when operating in this over-coupled region has not been well studied.

In this study, we model an implanted near-field WPT system and add bio-compatible material coating and tissue around the receiver as shown in Fig 1, where the design of the WPT system is based on the study presented by Sample et al. in [3]. The transmitter and receiver are symmetric, and each consists of a driven or load-connected loop, plus a resonant

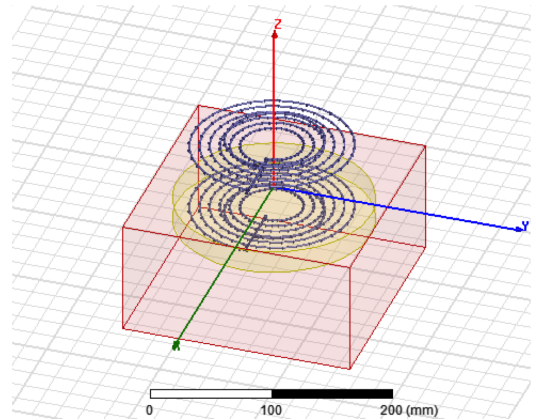


Fig. 1. A strongly-coupled WPT system with implanted receive coil is simulated to determine which of its two resonant modes results in lower SAR. The red box is a human tissue phantom, and the implanted receive coil is surrounded by a bio-compatible material shown in yellow.

coil with discrete tuning capacitors. The tissue that surrounds the receiver coil is modeled as a homogenous muscle for simplicity with parameters based on [4]. The Ansys HFSS EM simulation suite is used in this study and the model constructed is shown in Fig 1. We characterize the difference in the spatial distribution of SAR in both modes in the over-coupled region and conclude that the higher frequency resonant mode has a lower SAR distribution compared to that of the lower frequency resonant mode.

II. RELATED WORK

Research done by Christ *et al.* [5] evaluates human EM exposure for WPT systems when the transmit coil is in close proximity to a person. However, their model does not include the implanted receive coil. Park *et al.* studied the dosimetry of two self-resonant coils in the over-coupled region using a nearby phantom head model (TARO), and concluded that the lower frequency resonant mode is the best for lower SAR [6]. However, they compared SAR at only two locations near the coils and do not consider implanted coils. This paper will explore the entire volume of tissue, and will model a system with a fully implanted receive coil.

Though existing work has contributed valuable insight into human EM exposure for near-field WPT system, studies on human EM exposure which target the powering of implanted devices are lacking, as are explorations of the advantages and disadvantages of near-field WPT in the over-coupled region.

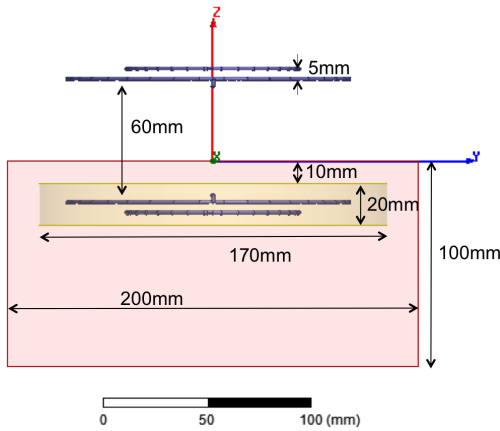


Fig. 2. The side view of the simulated system with scale labeled. The red box is a human tissue phantom, and the implanted receive coil is surrounded by a bio-compatible material shown in yellow.

III. DESIGN

A. Theory for Strongly Coupled Magnetic Resonator

The WPT configuration under test in this study is the pair of magnetically coupled resonators shown in Fig 1. At the critical coupling point, there is only one frequency at which the system attains peak efficiency. This is called the critical coupling frequency. As the distance between the transmitter and receiver is reduced, the frequency of peak efficiency starts to split into two modes; a lower frequency peak and a higher frequency peak. These modes diverge in frequency as coupling increases further. WPT efficiency optimization when peak frequency shifts can be achieved with fine tuning of the coils and capacitors, but this optimization is not performed in this study.

In the lower frequency mode, the H fields of the resonators are in phase; in the higher frequency mode, the resonator H fields are out of phase [6]. The resulting two modes can be understood by applying the coupling theory for microwave filters [7]. The coupling coefficient k which indicates the intensity of the coupling of the two resonators can be related by the two resonant frequencies as,

$$k = \frac{f_H^2 - f_L^2}{f_H^2 + f_L^2} \quad (1)$$

where f_L represents the lower resonant frequency and f_H represents the higher resonant frequency. In magnetically coupled resonator systems, if the coupling effect increases the stored magnetic flux, the resonant frequency shifts down from its critical-coupled frequency; otherwise, the resonant frequency shifts up from its critical-coupled frequency.

B. Modeling the Coils

The focus of this study is to analyze the characteristics of the SAR distribution of a strongly coupled resonant WPT system for the case where the receive coil is implanted. Thus, the modeling of the simulation includes a 4-coil WPT system and a human tissue phantom. Fig 2 shows the size and location of the model. The top loop-and-coil combination is the transmitter, and its location is swept vertically to achieve different

coil separation distances. The bottom receiver is enclosed by a cylinder of has a Polydimethylsiloxane (PDMS) coating surrounded, highlighted in light yellow in the figure. PDMS is a material often used in implants for its bio-compatible properties. Because the strongest E field of the magnetic resonator is located near the wire, this bio-isolation can also reduce the E field induced in tissue, which reduces SAR. This encapsulating bio-compatible cylinder has radius of 85mm and thickness of 20mm.

The operating frequency of the WPT system is designed near 13.56 MHz, because it is one of the ISM bands popularly used by WPT systems. However, in the over-coupled regime the two frequencies of peak efficiency will diverge, and therefore the frequency corresponding to maximum power transfer will be shifted away from the design frequency of 13.56 MHz. In this work, the coupling is adjusted such that the distance between the upper and lower peak efficiency frequencies is 4 MHz.

In HFSS, each turn of the coil and loop is modeled with 36 segment elements. Capacitors are modeled as lumped element to form resonance. The design parameters for the system are listed in Table I. The transmitter and receiver coils are symmetrically designed and the simulated result of $|S_{21}|^2$ (WPT efficiency) is 94% at critical coupling at 14.5 MHz. Because the topic of coil design for high efficiency is not within the scope of this paper, the details of how the coil system is designed are not included, but one can reference tuning techniques from [3].

TABLE I. PARAMETERS FOR COIL AND LOOP

Coil Parameters	Value
Coil inner radius (mm)	22
Number of turns	6
Change of radius (mm)	8.5
Wire radius (mm)	0.85
Tuning capacitor (pF)	33
Loop Parameters	Value
Radius (mm)	42
Tuning capacitor (pF)	660
Loop to coil Distance (mm)	5

C. Modeling the Tissue

The tissue is modeled as a homogenous muscle cube shown as the pink box in Fig 2, which has the dimension of 200mm×200mm×100mm. The frequency-dependent electrical parameters of muscle are listed in Table II [4] with density 1090 kg/m³ [8].

TABLE II. ELECTRICAL PARAMETERS OF MUSCLE

Frequency (MHz)	ϵ_r	$\tan\delta$	σ (S/m)
12.25	147.97	6.1922	0.6244
12.5	145.98	6.1582	0.62515
12.75	144.08	6.1244	0.62589
14.75	131.35	5.8575	0.63131
15	130.01	5.8249	0.63193
15.5	127.47	5.7603	0.63315

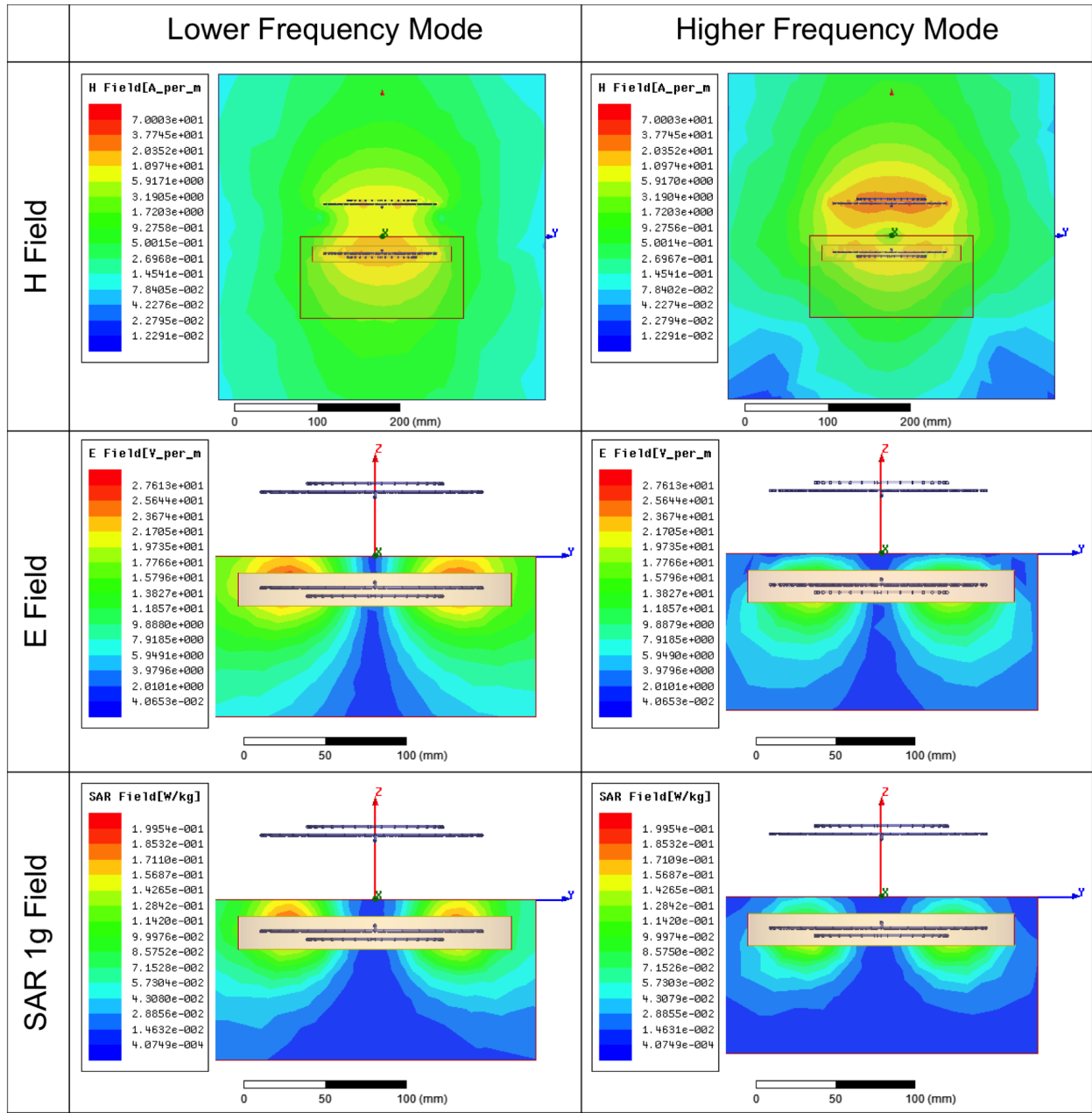


Fig. 3. The YZ-plane cross section of field patterns when the transmitter and receiver separation distance is 60mm with input power of 1W. They are, from top to bottom, H field, E field, and SAR 1g field. The left column shows the field patterns of the lower frequency mode, and the right column shows those of the higher frequency mode. The E field pattern is captured at phase=0; the H field pattern is captured at phase=90; the SAR plot is the average SAR over 1g of tissue. The axes of each field pair are scaled to be the same so that a visual comparison can be made between low and high frequency mode plots.

Even though it is more accurate to use an anatomical human body model [9] or tissue recipe for the WPT simulation in the 10 MHz band because different layers (such as skin, fat and muscle) of human body has different dielectric properties, it is reasonable to use a homogenous tissue model for this study because we intend to compare the different characteristics of the SAR distribution in one tissue type. HFSS computes SAR using the expression below:

$$\text{SAR} = \frac{\sigma E^2}{2\rho} \quad (2)$$

where σ is the electrical conductivity at a given frequency, and ρ is the mass density of the material, and E is the electric

field. The conductivity is defined in the equation below,

$$\sigma = \omega \epsilon_0 \epsilon_r \tan \delta \quad (3)$$

where the simulation parameters used are listed in Table II.

A large air box is placed to surround this system and acts as the radiation boundary, but it is not shown in Fig 2.

D. Simulation Setup

The system is modeled in HFSS using the Finite Element Method (FEM). The input port and the output port connecting the capacitor boundary and the loop are modeled as 50 Ω lumped ports. The basis function of the solution setup is

TABLE III. SAR COMPARISON WHEN VARYING DISTANCE AND RESONANT MODE

Dist (mm)	Freq (MHz)	S21 (dB)	Max SAR 1g (W/kg)	Max SAR 10g (W/kg)	Whole Tissue SAR	FOM
50	12.25	-2.39	0.232	0.198	3.80e-02	0.403
60	12.5	-2.79	0.200	0.166	3.33e-02	0.379
70	12.75	-3.67	0.150	0.122	2.52e-02	0.349
50	15.5	-1.64	0.177	0.133	1.76e-02	0.259
60	15	-2.26	0.155	0.116	1.65e-02	0.260
70	14.75	-3.12	0.147	0.111	1.61e-02	0.301

selected as zero order, because the coil size is much smaller than the wavelength. Finally, the frequency resolution is set to 0.125MHz.

IV. RESULT AND ANALYSIS

In all the simulations, the input source is set to a power level of 1 Watt. The SAR distribution for each of the two resonant modes is computed with three separation distances, 50mm, 60mm, and 70mm. The resulting distributions for the high and low frequency resonant modes are compared. Parameters including SAR 1g, SAR 10g and whole tissue SAR are collected in both resonant modes for the three locations (Table III). The efficiency in each test ($|S21|^2$) is also used as part of the figure of merit comparing the low frequency mode and high frequency mode. Because the efficiency for each case is different, it is not fair to compare the SAR value alone with different receive power levels. Thus, we define the figure of merit (FOM) using the normalized SAR and S21:

$$FOM = \frac{\text{normalized SAR}}{|S21|^2} \quad (4)$$

where normalized SAR is calculated by dividing SAR by the input power. In this way, either having a bad SAR performance or a low WPT efficiency will result in a large FOM, which is less desirable for an implanted WPT system. Fig 4 compares the FOM of the two modes at the three separation distances. It should be noted that, although the FOM is smaller as separation distance increases of the lower frequency mode, this does not necessarily mean that these are the preferred setup as the efficiency also decreases. However, as can be seen in the plot, the higher frequency mode is always better than the lower frequency mode for each separation distance.

Fig 3 shows the field patterns at the 60mm separation case, including H field, E field and SAR 1g. The left column represents the result of the lower frequency mode at 12.5 MHz and the right column shows the higher frequency mode at 15 MHz. The H field of the higher frequency mode has a null in the center compared to the lower frequency mode, which has the same result as that in [6]. The E field patterns inside the tissue are quite different between the modes. At the lower frequency mode, the location with the greater E field intensity is near the top of the tissue; whereas at the higher frequency mode, the higher intensity E field is located behind the receive coil. The SAR 1g field follows the same trend as the E field pattern. To compare the field pattern of each case more clearly, the axes are scaled to be the same, but both the peak E field and SAR 1g field have lower maxima in the higher frequency mode than in the lower frequency mode.

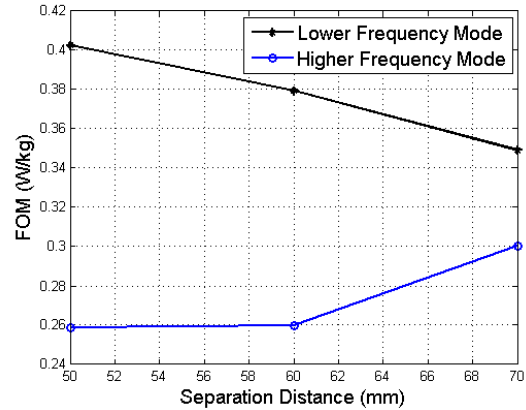


Fig. 4. Comparing the figure of merit of SAR at two modes with varying distance.

V. CONCLUSION

An implanted wireless power transfer system in the over-coupled regime was modeled and characterized in terms of SAR distribution which relates to tissue heating. The SAR distribution in the two resonant modes of the wireless power system were compared and the higher frequency mode was determined to be the best for reducing SAR levels, a key safety consideration for such systems. This result can guide future design of safe wireless power transfer systems.

VI. ACKNOWLEDGEMENTS

This work is supported by the National Science Foundation (NSF), EEC-1028725, CNS-1305072; the NSF Engineering Research Center (ERC) on Sensorimotor Neural Engineering, EEC-1028725; and the Paul G. Allen Family Foundation, Allen Distinguished Investigators program.

REFERENCES

- [1] ICNIRP, "Guidelines for limiting exposure to time-varying electric, magnetic and electromagnetic fields (up to 300 ghz)," 1998.
- [2] A. Sample, D. Meyer, and J. Smith, "Analysis, experimental results, and range adaptation of magnetically coupled resonators for wireless power transfer," *Industrial Electronics, IEEE Transactions on*, vol. 58, pp. 544–554, Feb 2011.
- [3] A. Sample, B. Waters, S. Wisdom, and J. Smith, "Enabling seamless wireless power delivery in dynamic environments," *Proceedings of the IEEE*, vol. 101, pp. 1343–1358, June 2013.
- [4] C. Gabriel, S. Gabriel, and E. Corthout, "The dielectric properties of biological tissues: I. literature survey," *Physics in Medicine and Biology*, vol. 41, no. 11, p. 2231, 1996.
- [5] A. Christ, M. Douglas, J. Roman, E. Cooper, A. Sample, B. Waters, J. Smith, and N. Kuster, "Evaluation of wireless resonant power transfer systems with human electromagnetic exposure limits," *Electromagnetic Compatibility, IEEE Transactions on*, vol. 55, pp. 265–274, April 2013.
- [6] S. Park, E. Kim, K. Wake, and S. Watanabe, "Dosimetry for two modes of resonance-based wireless power transfer system," in *Electromagnetic Compatibility, Tokyo (EMC'14/Tokyo), 2014 International Symposium on*, pp. 210–213, May 2014.
- [7] J. Hong and M. J. Lancaster, *Microstrip Filters for RF/Microwave Applications*. Wiley, 1st edition ed., 2001.
- [8] "Itis database for tissue properties." Accessed: Feb, 2015.
- [9] A. Christ, W. Kainz, E. G. Hahn, et al., "The virtual family—development of surface-based anatomical models of two adults and two children for dosimetric simulations," *Physics in Medicine and Biology*, vol. 55, no. 2, p. N23, 2010.